JOURNAL OF GEOPHYSICAL RESEARCH, VOL. 113, D12215, doi:10.1029/2007JD009372, 2008

Does the Madden-Julian Oscillation influence aerosol variability?

Baijun Tian,[1,2] Duane E. Waliser,[1] Ralph A. Kahn,[1,3] Qinbin Li,[1] Yuk L. Yung,[4] Tomasz Tyranowski,[4] Igor V. Geogdzhayev,[5] Michael I. Mishchenko,[5] Omar Torres,[6] and Alexander Smirnov[7]

Received 10 September 2007; revised 9 January 2008; accepted 18 February 2008; published 28 June 2008.

[1] We investigate the modulation of aerosols by the Madden-Julian Oscillation (MJO) using multiple, global satellite aerosol products: aerosol index (AI) from the Total Ozone Mapping Spectrometer (TOMS) on Nimbus-7, and aerosol optical thickness (AOT) from the Moderate Resolution Imaging Spectroradiometer (MODIS) on Terra and Aqua and the Advanced Very High Resolution Radiometer (AVHRR) on NOAA satellites. A composite MJO analysis indicates that large variations in the TOMS AI and MODIS/AVHRR AOT are found over the equatorial Indian and western Pacific Oceans where MJO convection is active, as well as the tropical Africa and Atlantic Ocean where MJO convection is weak but the background aerosol level is high. A strong inverse linear relationship between the TOMS AI and rainfall anomalies, but a weaker, less coherent positive correlation between the MODIS/AVHRR AOT and rainfall anomalies, were found. The MODIS/AVHRR pattern is consistent with ground-based Aerosol Robotic Network data. These results indicate that the MJO and its associated cloudiness, rainfall, and circulation variability systematically influence the variability in remote sensing aerosol retrieval results. Several physical and retrieval algorithmic factors that may contribute to the observed aerosol-rainfall relationships are discussed. Preliminary analysis indicates that cloud contamination in the aerosol retrievals is likely to be a major contributor to the observed relationships, although we cannot exclude possible contributions from other physical mechanisms. Future research is needed to fully understand these complex aerosol-rainfall relationships.

Citation: Tian, B., D. E. Waliser, R. A. Kahn, Q. Li, Y. L. Yung, T. Tyranowski, I. V. Geogdzhayev, M. I. Mishchenko, O. Torres, and A. Smirnov (2008), Does the Madden-Julian Oscillation influence aerosol variability?, *J. Geophys. Res.*, *113*, D12215, doi:10.1029/2007JD009372.

1. Introduction

[2] Atmospheric aerosols (mainly in the troposphere) play an important role in the climate system and the hydrologic cycle [*IPCC*, 2007; *Kaufman et al.*, 2002a; *Ramanathan et al.*, 2001; *Yu et al.*, 2006]. They interact directly with solar and thermal radiation by scattering sunlight and reflecting a fraction of it back to space, and by absorbing sunlight in the atmosphere in some cases. Thus aerosols can cool the climate system and surface, but may warm the atmosphere [e.g., *Charlson et al.*, 1992; *Eck et al.*, 1998; *Kiehl and Briegleb*, 1993; *Ramanathan et al.*, 2001; *Satheesh and Ramanathan*, 2000; *Twomey et al.*, 1984]. As a result, aerosols can influence the atmospheric temperature, water vapor profiles, and cloud development [e.g., *Ackerman et al.*, 2000; *Hansen et al.*, 1997] and in turn the hydrological cycle [e.g., *Ramanathan et al.*, 2001]. Aerosols also influence cloud droplet concentration and size by serving as cloud condensation nuclei (indirect effect) and may cause changes in precipitation patterns, cloud cover, and possibly the frequency of extreme events [e.g., *Andreae et al.*, 2004; *Kaufman and Koren*, 2006; *Koren et al.*, 2004; *Rosenfeld*, 1999, 2000].

[3] Unlike greenhouse gases, such as carbon dioxide and methane, which have long enough lifetimes to become rather homogeneous in the atmosphere, the spatial and temporal distributions of aerosols are heterogeneous owing to wet and dry deposition, which typically remove them from the atmosphere within about a week [*Herman et al.*, 1997; *Husar et al.*, 1997]. Thus daily global satellite observations and continuous in situ measurements are needed to document the variability of aerosol amounts

[1]Jet Propulsion Laboratory, California Institute of Technology, Pasadena, California, USA.
[2]Now at Joint Institute for Regional Earth System Science and Engineering, University of California, Los Angeles, California, USA.
[3]Now at NASA Goddard Space Flight Center, Greenbelt, Maryland, USA.
[4]Division of Geological and Planetary Sciences, California Institute of Technology, Pasadena, California, USA.
[5]NASA Goddard Institute for Space Studies, New York, New York, USA.
[6]Joint Center for Earth Systems Technology, University of Maryland Baltimore County, Baltimore, Maryland, USA.
[7]Sciences Systems and Applications, Inc., Lanham, Maryland, USA.

0148-0227/08/2007JD009372$09.00

and their optical properties over the globe [*Kaufman et al.*, 2002a; *King et al.*, 1999]. However, due to sampling issues, aerosol type discrimination, and other measurement challenges, the spatial and temporal variability of aerosols has not yet been comprehensively documented. In particular, to the best of our knowledge, the spatial and temporal patterns of intraseasonal (30–90 d) aerosol variability and its connection to the Madden-Julian Oscillation (MJO) have not yet been explored.

[4] The MJO (aka Intraseasonal Oscillation) [*Madden and Julian*, 1971, 1994, 2005] is the dominant component of intraseasonal variability in the tropical atmosphere. It is characterized by slow ($\sim$5 m s^{-1}) eastward-propagating, large-scale oscillations in the tropical deep convection and baroclinic winds, especially over the warmest tropical waters in the equatorial Indian and western Pacific Oceans [*Hendon and Salby*, 1994; *Kiladis et al.*, 2001; *Rui and Wang*, 1990]. Such characteristics tend to be most strongly exhibited during boreal winter (November–April), when the Indo-Pacific warm pool is centered near the equator. During boreal summer (May–October), the change in the large-scale circulation associated with the Asian summer monsoon tends to cause the large-scale aspects of the disturbances to propagate more northeastward, from the equatorial Indian Ocean into Southeast Asia [e.g., *Waliser*, 2006a; *Wang and Rui*, 1990]. *Lau and Waliser* [2005] and *Zhang* [2005] provide a comprehensive review of the MJO and related issues.

[5] Since its discovery, the MJO has remained a topic of significant interest, due to its wide-ranging interactions with the climate system, and the fact that it represents a connection between the better-understood weather and seasonal-to-interannual climate variations. To date, the MJO has been shown to have important influences on various physical weather and climate phenomena over the globe at many timescales, such as the diurnal cycle of tropical deep convection [e.g., *Tian et al.*, 2006a], Asian and Australian monsoon onsets and breaks [e.g., *Wheeler and McBride*, 2005], El Niño-Southern Oscillation [e.g., *Lau*, 2005], tropical hurricanes [e.g., *Maloney and Hartmann*, 2000], extreme precipitation events [e.g., *Jones et al.*, 2004], and extratropical circulation and its weather patterns [e.g., *Vecchi and Bond*, 2004]. Furthermore, the large-scale MJO convection, circulation and thermodynamic characteristics have also been relatively well documented and in some cases understood [e.g., *Hendon and Salby*, 1994; *Kiladis et al.*, 2001; *Rui and Wang*, 1990; *Tian et al.*, 2006b]. However, the impact of the MJO on atmospheric composition is only beginning to be documented [e.g., *Tian et al.*, 2007; *Wong and Dessler*, 2007]. In the present study, we use global satellite aerosol observations to investigate the possible modulation of aerosol by the MJO. Important to this work are the findings regarding the potential predictability of the MJO that extends to 2–4 weeks as indicated by empirical and dynamical studies [e.g., *Waliser*, 2006b]. If the MJO systematically influences aerosol variability, then societally relevant prediction of aerosols and air quality with similar lead times may be possible.

[6] Section 2 introduces the global satellite aerosol products used for this study, along with the methodology. Our main results are presented in section 3. Section 4 discusses the results and their interpretation, followed by concluding remarks in section 5.

2. Data and Methodology

[7] Numerous global aerosol products have been derived from satellite sensors. However, due to the challenge of retrieving aerosol parameters from top-of-atmosphere radiances, including issues related to sensor calibration, cloud screening, corrections for surface reflectivity and variability of aerosol properties (size distribution, refractive index, etc.) [*Kahn et al.*, 2007; *King et al.*, 1999], substantial differences exist among the global aerosol products [*Jeong and Li*, 2005b; *Jeong et al.*, 2005; *Myhre et al.*, 2004, 2005]. For this study, we use three satellite-derived global aerosol products: Total Ozone Mapping Spectrometer (TOMS) Aerosol Index (AI), Moderate Resolution Imaging Spectroradiometer (MODIS) aerosol optical thickness (AOT), and Global Aerosol Climatology Project (GACP)/Advanced Very High Resolution Radiometer (AVHRR) AOT. The use of multisatellite aerosol products will test the data dependence of our MJO-aerosol results. Furthermore, the similarities and differences of our MJO-aerosol results among different satellite aerosol products will help us understand the similarities and differences of the multisatellite aerosol products.

[8] The TOMS product used here is the daily AI (level 3, version 8) on a resolution 1° × 1.25° latitude-longitude made by the Nimbus-7 TOMS from January 1980 to December 1992 [*Herman et al.*, 1997]. Currently the AI is derived from observations by the Ozone Monitoring Instrument (OMI) onboard the Aura satellite [*Torres et al.*, 2007]. The AI is calculated from the ratio of ultraviolet (UV) radiance measurements at 0.331 and 0.360 μm, and can detect the UV-absorbing aerosols over both ocean and land [*Herman et al.*, 1997; *Hsu et al.*, 1996], even over very bright clouds and ice/snow surfaces [*Hsu et al.*, 1999a]. The AI is most sensitive to UV-absorbing aerosols such as mineral dust, elevated biomass burning smoke, and volcanic ash, and is insensitive to nonabsorbing aerosols, such as sea salt and sulfate aerosols [*de Graaf et al.*, 2005; *Torres et al.*, 1998]. Furthermore, the AI is highly dependent on the altitude of the aerosol layer and cannot detect biomass burning aerosols in the lower troposphere, below about 2 km, and any aerosols below cloud tops [*de Graaf et al.*, 2005; *Hsu et al.*, 1999b]. The magnitude of the AI depends on aerosol parameters, such as AOT, single-scattering albedo, and asymmetry parameter, and surface albedo. In particular, the AI increases linearly with AOT, at a rate proportional to the aerosol single-scattering albedo [*de Graaf et al.*, 2005; *Torres et al.*, 1998]. The field of view of the TOMS instrument is large, about 50 × 50 km at nadir, and 150 × 250 km at the extreme off nadir. Thus large amounts of subpixel clouds may exits and contaminate the TOMS AI retrieval, masking the absorption signal of any aerosols that may occur below the clouds.

[9] MODIS, aboard the NASA Earth Observing System's Terra and Aqua satellites (crossing the equator in opposite directions at about 10:30 and 13:30 local time, respectively), retrieves total-column AOT at 10-km resolution from near-global daily observations. Different retrieval algorithms are

applied over ocean and land. Over ocean, MODIS utilizes calibrated radiances observed in six bands (nominal wavelengths of 0.55, 0.66, 0.87, 1.24, 1.64, and 2.13 μm) at a spatial resolution of 0.5 km under clear-sky conditions determined by a dedicated cloud-masking algorithm [*Li et al.*, 2004; *Martins et al.*, 2002] to retrieve aerosol properties [*Levy et al.*, 2003; *Remer et al.*, 2005; *Tanre et al.*, 1997]. Because of its wide spectral range and the greater simplicity of the ocean surface, the MODIS retrieved AOT over ocean has greater accuracy (±0.03) [*Levy et al.*, 2003, 2005; *Remer et al.*, 2002, 2005]. The over-land MODIS aerosol algorithm utilizes calibrated radiances observed in three bands (nominal wavelengths of 0.47, 0.66, and 2.13 μm) [*Kaufman et al.*, 1997; *Remer et al.*, 2005]. Over vegetated land, MODIS retrieves AOT with high accuracy (±0.05) [*Chu et al.*, 2002; *Remer et al.*, 2005]. The MODIS AOT employed in this study is the L3 MOD08 data product, Version 4, reported at 0.55 μm, on $1^\circ \times 1^\circ$ spatial grids, and from 24 February 2000 to 9 December 2005.

[10] The GACP/AVHRR (hereafter AVHRR) aerosol product [*Geogdzhayev et al.*, 2002; *Mishchenko et al.*, 1999; *Mishchenko and Geogdzhayev*, 2007] (updated at http://gacp.giss.nasa.gov/) contains the daily mean AOT at 0.55 μm from 1 January 1982 to 30 June 2005, over ocean. The product resolution is $1^\circ \times 1^\circ$ on an equal-angle grid. It is derived from clear-sky calibrated AVHRR channel 1 (nominal wavelength, $\lambda = 0.63$ μm) and channel 2 ($\lambda = 0.85$ μm) radiances, contained in the International Satellite Cloud Climatology Project (ISCCP) DX data set [*Rossow and Schiffer*, 1999]. The spatial resolution of the product is 30 km aggregated from AVHRR global area coverage data with 4-km resolution sampled from the 1-km raw data.

[11] There are several important differences between the TOMS AI and MODIS/AVHRR AOT. First, the TOMS AI is based on UV absorption by aerosols, thus most sensitive to absorbing aerosols and insensitive to nonabsorbing aerosols. On the other hand, The MODIS/AVHRR AOT, based on scattered light measurements, are sensitive to both absorbing and nonabsorbing aerosols. Second, the TOMS AI is insensitive even to absorbing aerosols in the lowest few kilometers of the troposphere, while the MODIS and AVHRR AOT are sensitive to the aerosols in the entire atmospheric column. It is important to note that the AOT from MODIS and AVHRR is a vertically integrated quantity reporting the magnitude of aerosol extinction based on measurements of aerosol scattering. Therefore any factors affecting the aerosol scattering and absorption efficiencies (e.g., size distribution and composition) and mass loading, such as wet deposition, atmospheric relative humidity (RH), surface wind speed, and biological production, impact the retrieved AOT value. Third, the field of view or pixel of the TOMS instrument is very coarse (50 km at nadir), whereas it is much finer for MODIS (0.5 km at nadir) and AVHRR (1 km at nadir). Thus MODIS and AVHRR AOT are more effective at screening clouds, and may be able to detect the aerosols between broken clouds. Fourth, the MODIS and AVHRR AOT can only measure aerosols in the "cloud-free" regions as determined by their cloud clearing algorithms. On the other hand, the TOMS AI can detect aerosols above cloud tops, provided the scene at 50 km scales is sufficiently uniform. All the differences discussed above can result in sampling biases that need to be considered when interpreting the results from TOMS AI and MODIS/AVHRR AOT. Fifth, the cloud contamination effects are different for the TOMS AI and MODIS/AVHRR AOT due to their different pixel resolutions, cloud clearing algorithms and fundamental retrieval methods. The MODIS/AVHRR aerosol retrievals are based on scattered light measurements. There are two ways that clouds affect these retrievals: (1) the existence of subpixel sized clouds or very thin cirrus in pixels identified as cloud-free [*Kaufman et al.*, 2005; *Zhang et al.*, 2005] and (2) enhanced illumination of the cloud-free column through the reflection of sunlight by nearby clouds, also called as "cloud adjacency effect" [*Kaufman et al.*, 2005; *Wen et al.*, 2001, 2006, 2007; A. Marshak et al., A simple model for the cloud adjacency effect and the apparent bluing of aerosols near clouds, submitted to *Journal of Geophysical Research*, 2007]. Both these effects produce anomalously high AOT retrieval results. In contrast, the TOMS AI is based on UV absorption by aerosols. Unscreened subpixel clouds above any absorbing aerosol layers within the relatively large ($\sim$ 50 km) TOMS pixels would scatter light, homogenizing the radiation field, and reducing the particle UV absorption signal used to detect aerosols in this method, producing an anomalously low AI retrieval result.

[12] To help validate and understand the relationships between the MJO rainfall and satellite aerosol products, we also use the V2.0, L2.0 (cloud-screened and quality-assured) daily Aerosol Robotic Network (AERONET) AOT at Kaashidhoo (73.5°E, 4.9°N) in the equatorial Indian Ocean and Nauru (167°E, 0.5°S) in the equatorial Western Pacific. The AERONET program [*Holben et al.*, 1998, 2001] is a federated, ground-based aerosol measurement network using automatic sun and sky scanning spectral radiometers. AERONET includes about 200 sites around the world, covering all major tropospheric aerosol regimes. Spectral radiance measurements are calibrated and screened for cloud-free conditions [*Smirnov et al.*, 2000]. The program provides quality-assured aerosol optical properties to assess and validate satellite retrievals [*Holben et al.*, 2006]. The AERONET AOT data used here from Kaashidhoo were taken between 20 February 1998 and 11 July 2000, and those for Nauru are from 15 June 1999 to 11 June 2006.

[13] To identify MJO events, we use global pentad (i.e., 5-d average) rainfall data from the NOAA Climate Prediction Center (CPC) Merged Analysis of Precipitation (CMAP, *Xie and Arkin* [1997]) from 1 January 1979 to 31 May 2006 on a $2.5^\circ \times 2.5^\circ$ grid. For the MJO analysis and composite procedure, we use the approach described in our previous work [e.g., *Tian et al.*, 2006b; *Waliser et al.*, 2003]. Briefly, all the data were first binned into pentad values. Intraseasonal anomalies were obtained by removing the annual cycle, and then filtering the data with a 30–90 d band pass. To isolate the dominant structure of the MJO, an extended empirical orthogonal function (EEOF) [*Weare and Nasstrom*, 1982] was applied using time lags of ±5 pentads (i.e., 11 pentads total) on boreal winter rainfall for the region 30°S–30°N and 30°E–150°W [see *Tian et al.*, 2006b, Figure 1]. Next, MJO events were chosen based on the amplitude time series of the first EEOF mode of the rainfall anomaly. Figure 1 shows the dates and number of the selected MJO events, along with an indication of their relative amplitudes. For each selected MJO event, the

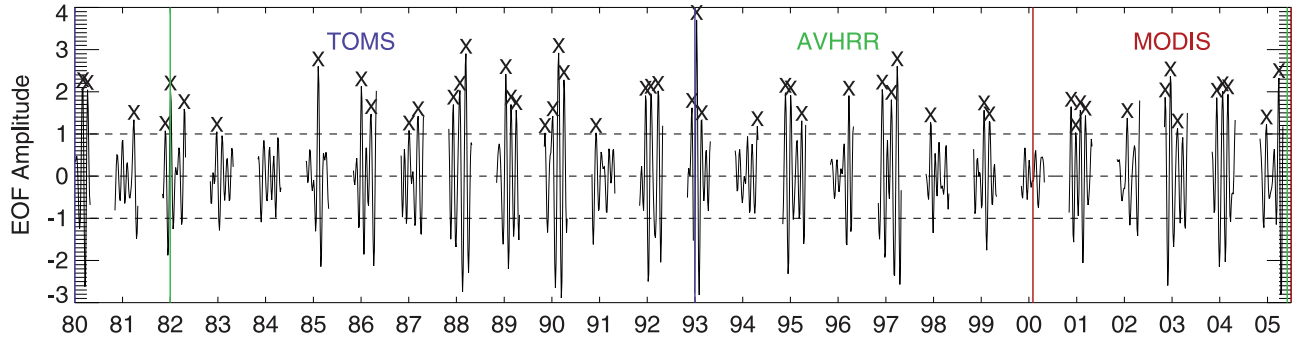

Figure 1. Dates (indicated by x) of selected MJO events for TOMS (26, from January 1980 to December 1992), MODIS (13, from February 2000 to June 2005), and AVHRR (48, from January 1982 to May 2005) periods based on the amplitude pentad time series for the first EEOF mode of CMAP rainfall anomaly from NH wintertime (November–April) and the region 30°S–30°N and 30°E–150°W. Three dashed lines show the EEOF amplitude of ±1 and 0. The solid colored lines indicate the start and end of each aerosol data record (blue for TOMS, red for MODIS, and green for AVHRR).

corresponding 11-pentad rainfall, AI or AOT anomalies were extracted for each data set (TOMS, MODIS, AVHRR, and AERONET). A composite MJO cycle (11 pentads) of anomalies was then obtained by averaging the selected MJO events.

3. Results

[14] Figure 2 shows the horizontal maps of the TOMS AI anomalies for the composite MJO cycle with 95% confidence limits applied based on a Student's t-test. For simplicity, only lags ±4, ±2, and 0 pentads of the MJO cycle are shown. Contour plots overlaid on the color shadings are the corresponding MJO composite rainfall anomalies. The AI anomalies range up to about ±0.6 for the *composite* MJO but about ±2 for individual events. This indicates that intraseasonal AI variations are significant and comparable to those associated with the annual cycle and interannual variability [e.g., *Cakmur et al.*, 2001; *Herman et al.*, 1997; *Mahowald et al.*, 2003]. Figure 2 shows that significant AI anomalies are found in the tropical Indian and western Pacific Oceans where the MJO convection is active. Evident in Figure 2 is the close association between negative AI anomalies and positive rainfall anomalies and vice versa. The zero-lag correlation between AI and rainfall is shown in Figure 3 (top), which illustrates a strong anticorrelation between TOMS AI and rainfall in the tropical Indian and western Pacific Oceans. This relationship seems to be consistent with the seasonal study of *Lau and Kim* [2006], who shows a decrease of TOMS AI after the Indian summer monsoon was established (high rainfall) (their Figure 2). Over equatorial Africa and Atlantic Ocean where MJO convection is relatively weak, equally large AI anomalies are also found in conjunction with relatively weak rainfall anomalies from the MJO. The correlation between AI and rainfall is also negative over this region albeit much weaker. The large AI anomalies over this region may be due to the large background AI, that is, high absorbing aerosol loading due to Sahara desert dust and biomass burning smoke from South Africa [*Herman et al.*, 1997].

[15] A diagram similar to Figure 2, but for the MODIS AOT, is shown in Figure 4. The MODIS AOT anomalies range up to about ±0.02 for the composite MJO but about ±0.1 for individual events. These intraseasonal variations are large compared to their background mean (∼0.2) [*Jeong et al.*, 2005; *Myhre et al.*, 2004, 2005] and its uncertainty (±0.03) [*Remer et al.*, 2005]. Similar to TOMS AI, significant MODIS AOT anomalies are also found in the tropical Indian and western Pacific Oceans as well as equatorial Africa and Atlantic Ocean. However, the relationship between MODIS AOT and rainfall is less coherent than for TOMS AI. In general, in the tropical Indian and western Pacific Oceans where the MJO convection is active, positive AOT anomalies tend to be associated with positive rainfall anomalies and vice versa. This is also confirmed by a weak positive correlation between MODIS AOT and rainfall in this region (Figure 3, middle). Our results appear to be consistent with the positive correlation between the MODIS AOT and cloud cover found by *Kaufman et al.* [2002b, 2005], *Loeb and Manalo-Smith* [2005], *Zhang et al.* [2005], *Matheson et al.* [2005], and *Lin et al.* [2006].

[16] The spatial and temporal pattern of the AVHRR AOT anomalies is similar to that for MODIS, though it is even less coherent (not shown). This is probably due to the poorer spatial coverage of the daily AVHRR AOT data and its smaller "dynamic range." More conservative cloud screening algorithms were applied by *Mishchenko et al.* [1999] and *Geogdzhayev et al.* [2002], in addition to the ISCCP cloud detection algorithm [*Rossow and Garder*, 1993]. The additional cloud screening aims to eliminate small cumulus clouds and optically thin cirrus clouds. However, the strict cloud masking may have the adverse impact of discarding real aerosol signals by misclassifying them as clouds [*Haywood et al.*, 2001; *Husar et al.*, 1997]. For instance, an AOT threshold of 2 is used for the GACP/AVHRR product as a part of cloud screening, which will discard some cases with heavy aerosol loading [*Mishchenko and Geogdzhayev*, 2007]. The less coherent AVHRR AOT MJO variability is also consistent with an even weaker positive correlation between AVHRR AOT and rainfall, relative to MODIS (Figure 3, bottom). Our results appear to be consistent with the positive correlation between the AVHRR AOT and cloud cover found by *Ignatov and Nalli* [2002] and *Ignatov et al.* [2004].

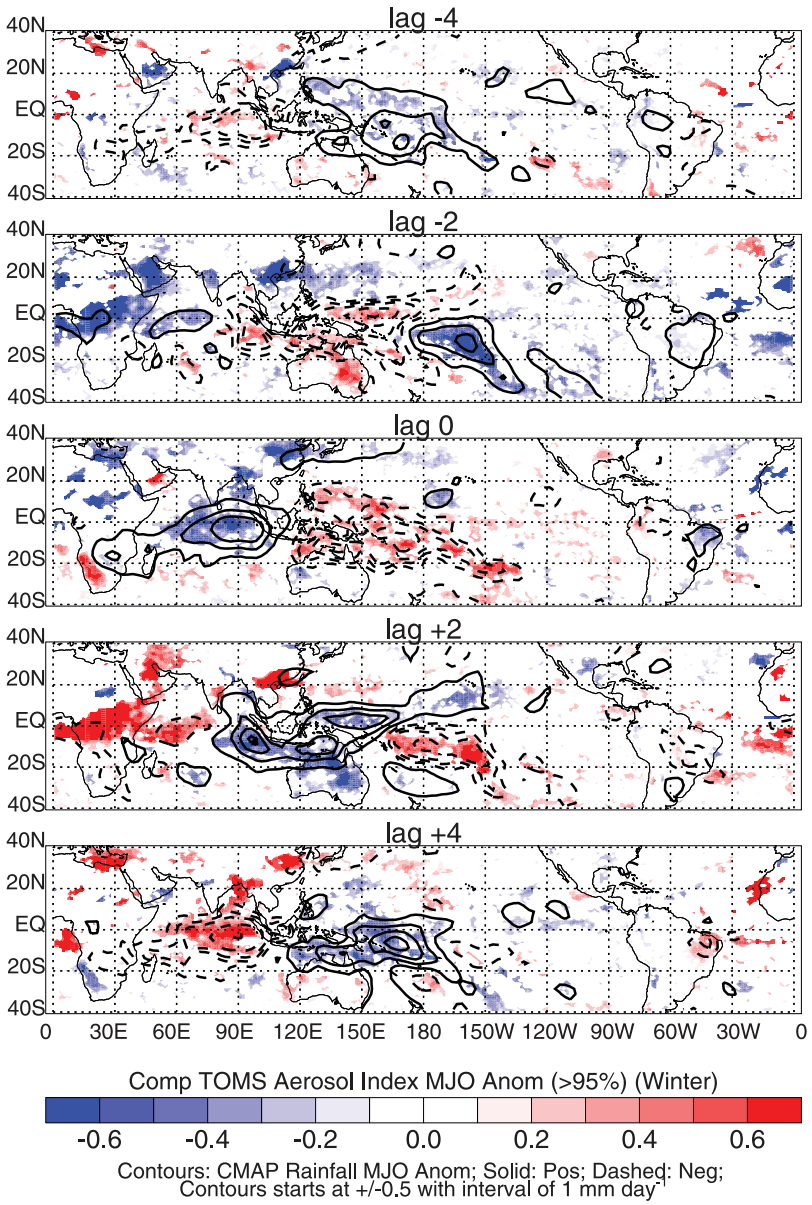

Figure 2. Composite maps of the TOMS AI anomalies (color shading) associated with the MJO indicated by the CMAP rainfall anomalies (contours). TOMS AI anomalies are only plotted if they exceed 95% confidence limit using a Student's t-test.

[17] In an attempt to gain deeper understanding of the above (apparent) discrepancy in the satellite-observed aerosol anomalies associated with the MJO, the relationship between the composite AERONET AOT and rainfall anomalies at Kaashidhoo and Nauru was examined (Figure 5). We present the AERONET AOT at 0.50 μm, which is close to the channel used by MODIS and AVHRR, though the results for other channels are similar (not shown). For comparison, time series from the composite TOMS AI, MODIS AOT, and AVHRR AOT near these two sites are also shown in Figure 5. Consistent with the discussion above, the TOMS AI is negatively correlated with rainfall, whereas the MODIS/AVHRR AOT is positively correlated with rainfall at both Kaashidhoo and Nauru. A strong positive correlation exists between the AERONET AOT and rainfall anomalies at both Kaashidhoo and Nauru (correlation coefficient $\sim$ +0.70 for Kaashidhoo and +0.90 for Nauru). This aerosol-rainfall relationship appears to be consistent with the positive correlation between AERONET AOT and cloud cover found by *Jeong and Li* [2005a]. Furthermore, the magnitude of the AERONET AOT anomalies ($\sim$0.02) is comparable to that for the MODIS/AVHRR AOT anomalies. Thus the AERONET data seem to support the weak positive correlation between MODIS/AVHRR AOT and rainfall anomalies shown in Figures 3 and 4.

4. Discussion

[18] The findings described above raise a number of questions. Why is there a negative correlation between the TOMS AI and rainfall anomalies but a positive correlation

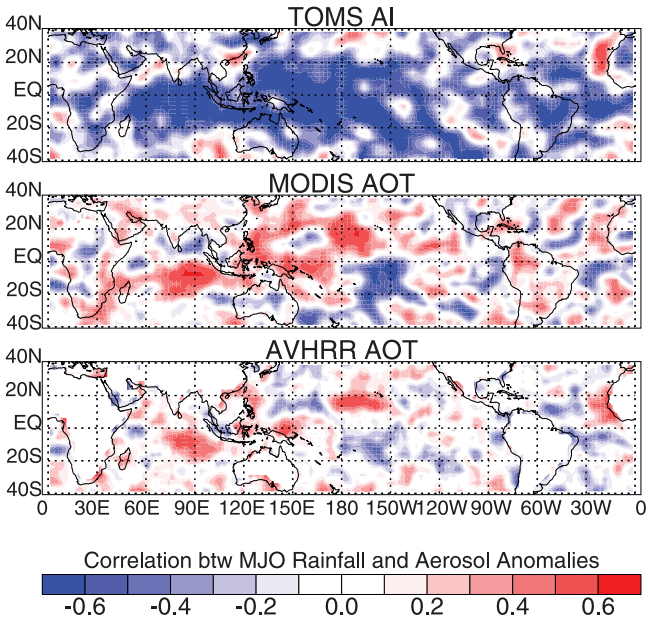

Figure 3. Zero-lag correlation between the MJO composite CMAP rainfall anomalies and aerosol anomalies (shown in Figures 2 and 4) from the three satellite aerosol products (i.e., TOMS AI, MODIS AOT, and AVHRR AOT).

between the MODIS/AVHRR AOT and rainfall anomalies? Are these aerosol-rainfall relationships physical, or is one or more of them a result of the aerosol sampling and retrieval artifacts? Similar aerosol-cloud cover relationships, at timescales other than intraseasonal, have been reported in the literature, such as *Ignatov and Nalli* [2002], *Ignatov et al.* [2004], *Jeong and Li* [2005a, 2005b], *Jeong et al.* [2005], *Kaufman et al.* [2002b, 2005], *Lau and Kim* [2006], *Loeb and Manalo-Smith* [2005], *Lin et al.* [2006], *Matheson et al.* [2005], *Myhre et al.* [2004, 2005], and *Zhang et al.* [2005]. However, the reasons for this aerosol-rainfall (cloud cover) relationship are still unclear. Possible reasons include: aerosol humidification effect (AHE) or aerosol growth, wet deposition, low-level wind effect (including both advection and speed), biological production, sampling effect, and cloud contamination. In the next few paragraphs, we discuss the manner in which these mechanisms may contribute to the observed aerosol-rainfall relationships.

[19] First, some aerosol types are hygroscopic, meaning that they grow in the presence of humid conditions. As a result, their size increases and their refractive indices change, that in turn leads to changes in their optical properties and increase of AOT. This dependence of AOT on the atmospheric RH is referred to as AHE or aerosol growth [e.g., *Jeong et al.*, 2007]. This growth mechanism is usually large for scattering aerosols, such as sulfate aerosols and sea salts. For example, the scattering cross section of sulfate aerosols doubles as RH increases from 40% to 80% [*Hobbs et al.*, 1997; *Kaufman et al.*, 1998]. On the other hand, the growth of the absorbing aerosols, to which TOMS AI is sensitive, with increasing RH should be much smaller than that for the scattering aerosols, to which MODIS/AVHRR is sensitive [*Redemann et al.*, 2001]. RH throughout most of the tropospheric column is much higher in the wet phase of the MJO (~80%) than its dry phase (~30%) [e.g., *Chen et al.*, 1996; *Lin and Johnson*, 1996]. Therefore the AHE may contribute to the positive correlation between the rainfall and MODIS/AVHRR AOT (a measure of aerosol scattering). However, the AHE would be expected to have a negligible effect on TOMS AI (which measures only absorbing aerosol).

[20] Second, rainfall is a highly efficient aerosol removal mechanism through wet deposition [e.g., *Koch et al.*, 2003; *Wilcox and Ramanathan*, 2004]. In the wet phase of the MJO, the precipitation is significantly enhanced and this can increase the wet deposition and reduce the aerosol mass loading in the troposphere. The opposite is true for the dry phase of the MJO. Thus the wet deposition could contribute to the negative correlation between the TOMS AI and rainfall, but it cannot explain the positive correlation between MODIS/AVHRR AOT and rainfall. Furthermore, if wet deposition is important, it should affect the MODIS/AVHRR AOT more than the TOMS AI, because (1) near-surface aerosols (detected by MODIS and AVHRR AOT) are much more susceptible to rainout than elevated aerosols (detected by TOMS AI), and (2) nonabsorbing aerosols (detected by MODIS/AVHRR AOT) tend to be more hygroscopic and more likely captured by rain. Therefore if wet deposition is contributing to the negative correlation between rainfall and aerosol in the TOMS retrievals, there have to be additional mechanisms that overcome this influence in order for the MODIS/AVHRR to exhibit a (weak) positive correlation with rainfall.

[21] Third, low-level wind variability including both wind advection and wind speed is another important factor influencing the near-surface aerosol variability, especially over ocean [e.g., *Chapman et al.*, 2002; *Jeong and Li*, 2005b; *Smirnov et al.*, 2003]. For example, *Smirnov et al.* [2003] found a link between directly measured aerosol optical parameters from AERONET and 24-h averaged surface wind speed at Midway Island in the central Pacific Ocean. Increased wind speed enhances the emission of relatively large sea-salt aerosols, which influences the AOT most strongly at infrared wavelengths. Also, *Chapman et al.* [2002] showed that dimethylsulphide (DMS) fluxes from the ocean to the atmosphere increase under stronger wind conditions. The DMS, through oxidization, can transform into sulfate aerosols, which have important implications for climate [*Charlson et al.*, 1987]. The stronger surface wind speed associated with the westerly wind bursts during the wet phase of the MJO [e.g., *Kiladis et al.*, 1994, 2005] may generate more bright, near-surface sea salts and increase low-level sulfate aerosol through increasing the DMS flux from the ocean to the atmosphere. These low-level strong scattering sea salts and sulfate aerosol can only be detected by MODIS/AVHRR AOT but not by TOMS AI. Thus the ocean surface wind speed anomalies associated with the MJO may contribute to the positive correlation between MODIS/AVHRR AOT and rainfall, albeit no influence on the negative relationship between TOMS AI and rainfall is expected. Furthermore, *Jeong and Li* [2005b] show that the high AVHRR AOT plume over the Atlantic is clearly associated with the low-level wind vector. The high MODIS/AVHRR AOT MJO anomalies over the Atlantic (Figures 2 and 4) may be induced by the low-level

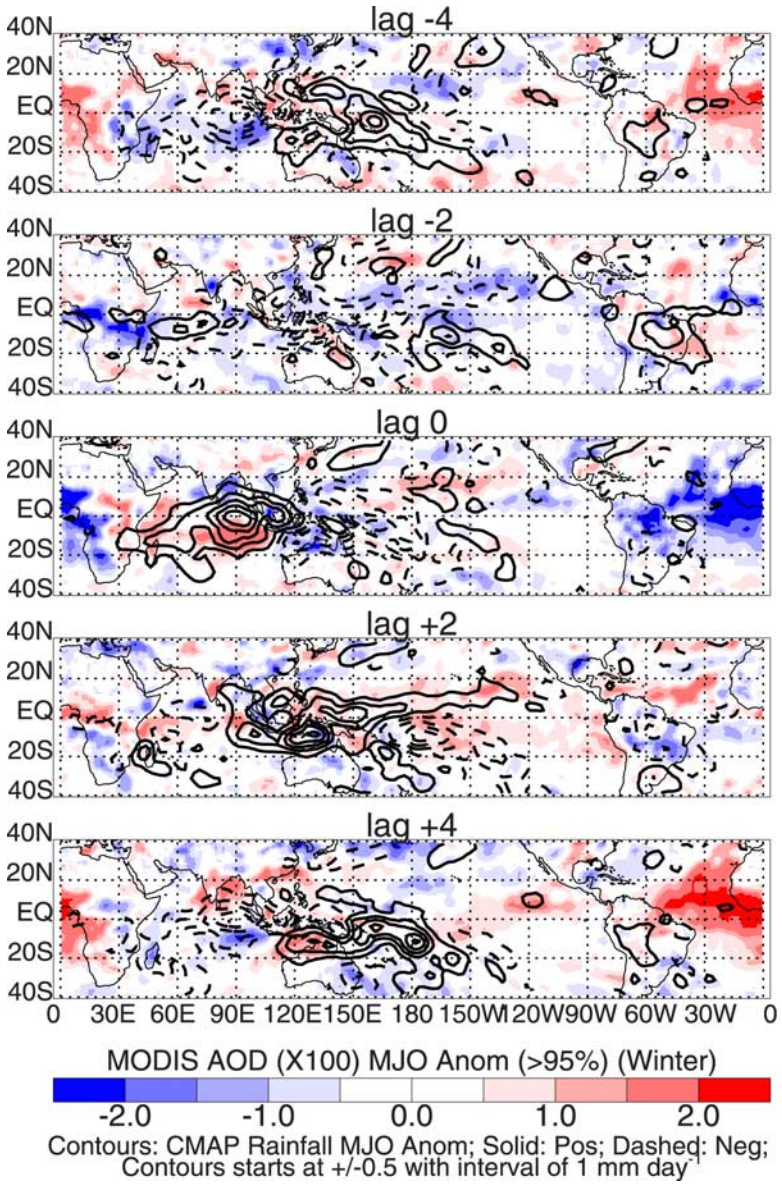

Figure 4. As in Figure 2, except for MODIS AOT.

easterlies or westerlies over the Atlantic, generated by the MJO convection over the western Pacific [e.g., *Hendon and Salby*, 1994]. Also, during the wet phase of the MJO, strong low-level mass convergence associated with the MJO [*Kiladis et al.*, 2005; *Lin et al.*, 2005] may cause a build-up of low-level aerosols (thus AOT), which may also contribute to the positive correlation between MODIS/AVHRR AOT and rainfall.

[22] Another factor, which can contribute to the positive correlation between the MODIS/AVHRR AOT and rainfall, is phytoplankton variations associated with the MJO. *Jeong and Li* [2005b] show a positive correlation between long-term monthly mean AOT and ocean surface chlorophyll concentration in several regions (their Figure 10). Planktonic algae produce DMS and then, through oxidization, the DMS transforms into sulfate aerosols. Meanwhile, *Waliser et al.* [2005] show that the MJO produces systematic and significant variations in the ocean surface chlorophyll in a number of regions across the tropical Indian and Pacific Oceans, including the northern Indian Ocean, a broad expanse of the northwestern/central tropical Pacific Ocean, and a number of near-coastal areas in the far eastern Pacific Ocean. Interestingly, the MJO-related chlorophyll anomaly pattern is very similar to the MJO-related AVHRR AOT pattern. Thus the MJO may influence the aerosol variability, especially the scattering ones detected by MODIS and AVHRR, through its influence on oceanic biological production. However, it is also possible that the change in ocean color due to high chlorophyll concentrations may cause an overestimation of AOT.

[23] The above relationships and mechanisms provide plausible physical scenarios by which the aerosol-rainfall relationships reported here could all be consistent. For example, the negative aerosol-rainfall relationship exhibited by TOMS AI could be driven to the first order by wet deposition. Although this mechanism would also be acting

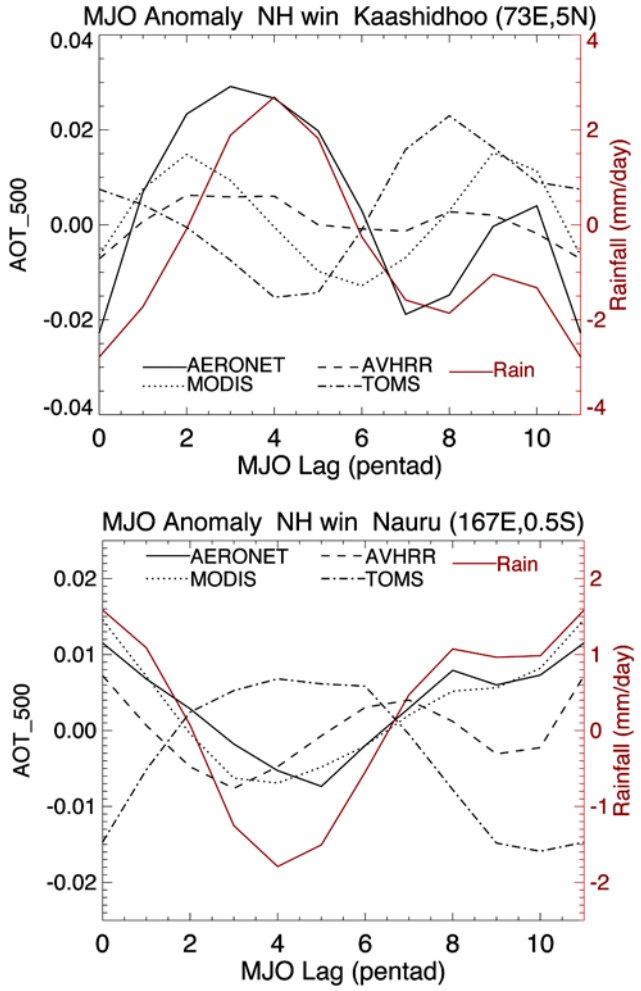

Figure 5. MJO composite CMAP rainfall anomalies and AERONET AOT at two AERONET sites: Kaashidhoo and Nauru. The TOMS AI, MODIS AOT, and AVHRR AOT at the nearby grids are also included for comparison.

on the MODIS/AVHRR AOT, these retrievals could also be effected by the AHE, low-level wind variability (advection and speed), which if strong enough, could change the sign of the aerosol-rainfall relationship to a weak positive one.

[24] However, these aerosol-rainfall relationships are also likely a result of the aerosol sampling artifacts associated with clouds and cloud-clearing procedures. As discussed above, the cloud tops and unscreened subpixel clouds could result in a negative bias in the TOMS AI. During the wet phase of the MJO, the amount of high cloud increases and cloud tops become higher; this can increase the negative bias in TOMS AI and produce negative correlations between TOMS AI and rainfall. For the MODIS and AVHRR, both the subpixel cloud contamination and cloud adjacency effect can lead to significant overestimation of the AOT. Thus the increased cloud amount during the wet phase of the MJO may increase the subpixel cloud contamination and cloud adjacency effect, which would contribute to the positive correlation between the MODIS/AVHRR AOT and rainfall. In addition, given the manner that AERONET performs cloud clearing (i.e., it interprets low variability across three samples as cloud free [*Smirnov et al.*, 2000]), it is possible that cloud contamination may contribute to the AERONET result too.

[25] To examine the possible role of cloud contamination in the positive correlation between MODIS/AVHRR AOT and rainfall, we performed a similar analysis to Figure 5, but based on the daily AOT data at Kaashidhoo that are computed from the direct sun measurement only around the time of successful almucantar measurements. The almucantar retrieval algorithm uses symmetry in sky-scan radiances for cloud detection [*Holben et al.*, 2006], which is a considerably more sensitive test, especially for thin cloud, than the three-sample variability method used in the direct-sun AOT algorithm. The result (Figure 6) indicates that there is no coherent positive correlation between the AOT and rainfall (with a correlation coefficient of −0.03) when the AERONET AOT data are filtered with the radiance symmetry cloud mask. This implies that the positive correlation between the AERONET AOT and rainfall anomalies in Figure 5 may be due to the cloud contamination effect. The same may be true for the weak positive correlation between the MODIS/AVHRR AOT and rainfall anomalies. Since the cloud contamination problem applies not only to the intraseasonal timescale but also other timescales, the cloud contamination may also partly contribute to observed cloud-aerosol relationships at other timescales as reported in previous studies based on satellite aerosol retrievals in the vicinity of clouds (see reference list in the first paragraph of this section).

5. Conclusions

[26] We investigated the possible modulation of the aerosol variability by the MJO using the TOMS AI, MODIS AOT, and AVHRR AOT global satellite aerosol products. Our results indicate that the intraseasonal aerosol variability is large and comparable to that associated with the annual cycle and interannual variability. Large variations in the

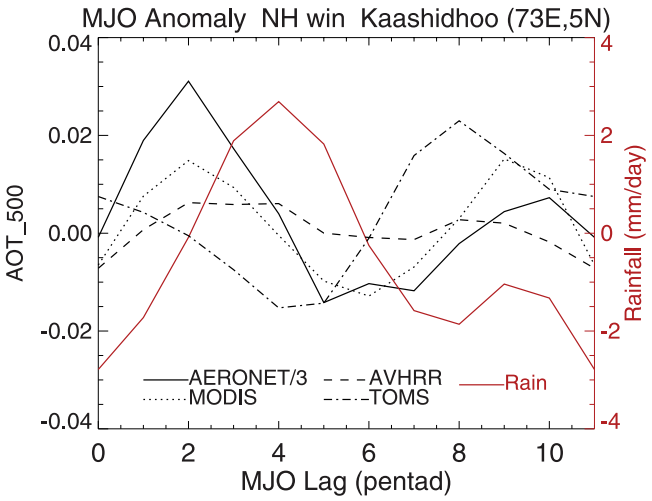

Figure 6. As in Figure 5, except for AERONET AOT at Kaashidhoo and obtained only around the time of almucantar measurement, that is, in the conditions when the sky was relatively clear and sky-scan symmetry was sufficiently uniform.

TOMS AI, MODIS AOT and AVHRR AOT are found mainly over the equatorial Indian and western Pacific oceans, where MJO convection is active, as well as tropical Africa and the Atlantic Ocean, where MJO convection is relatively weak but the background aerosol level is relatively high. In particular, there are systematic relationships between the TOMS AI, MODIS AOT, and AVHRR AOT anomalies and the MJO rainfall anomalies over the equatorial Indian and western Pacific oceans. During the wet phase of the MJO, TOMS AI decreases, whereas MODIS and AVHRR AOT increase, in association with the enhanced precipitation, cloud cover, and water vapor in the atmosphere, and vice versa. Thus there is a strong negative correlation between the TOMS AI and rainfall anomalies but a weaker and less coherent positive correlation between the MODIS AOT, AVHRR AOT and rainfall anomalies. The MODIS and AVHRR pattern is consistent with ground-based AERONET AOT data, which also show a significant positive correlation with rainfall anomalies at both Kaashidhoo and Nauru. These results indicate that the MJO and its associated cloudiness, rainfall, and circulation variability systematically influence the variability in remote sensing aerosol retrieval results.

[27] Numerous physical mechanisms, such as AHE, wet deposition, low-level wind variability (advection and speed), and biological production, and nonphysical mechanisms, such as different sensor sensitivities (absorbing versus nonabsorbing aerosols and upper versus lower tropospheric aerosols), sampling issue, and cloud contamination, may contribute to the observed aerosol-rainfall relationship. It is quite plausible that all these processes are acting to some degree. Preliminary analysis indicates that cloud contamination in the aerosol retrievals is likely to be a major contributor to the observed positive correlation between the MODIS/AVHRR/AERONET AOT and rainfall anomalies. However, we cannot exclude possible contributions from other physical mechanisms, based on the work presented here.

[28] This strong but complex relationship between the MJO and the aerosol variability, coupled with (1) the potential to predict the MJO with lead times up to 2–4 weeks [*Waliser*, 2006b], (2) the importance of understanding cloud clearing methods in aerosol remote sensing [e.g., *Kaufman et al.*, 2005; *Wen et al.*, 2007; *Zhang et al.*, 2005], (3) the important role of aerosol indirect effect on climate [e.g., *Andreae et al.*, 2004; *IPCC*, 2007; *Koren et al.*, 2004; *Ramanathan et al.*, 2001], suggests an important need to more completely document the aerosol intraseasonal variability as well as to further investigate the complex mechanisms behind the MJO rainfall and remotely sensed aerosol relationships documented here. To that end, a synergetic approach combining multisensor satellite data analysis, in situ and targeted aircraft observations, and state-of-the-art chemistry-transport modeling together will likely be required.

[29] **Acknowledgments.** This research was performed at the Jet Propulsion Laboratory (JPL), California Institute of Technology (Caltech), under a contract with NASA. B. Tian and D. Waliser were jointly supported by the Research and Technology Development program, Human Resources Development fund, and AIRS project at JPL as well as NASA Modeling, Analysis and Prediction program. The work of R. Kahn was supported in part by NASA Climate and Radiation Research and Analysis program, under H. Maring, and in part by the EOS-MISR instrument project. Y. Yung was supported by NASA grant NNG04GD76G to Caltech and T. Tyranowski acknowledges support by the Caltech SURF program in 2006. We also want to thank Eric Fetzer, Jianglong Zhang, and three anonymous reviewers for constructive comments and many scientists at the 2007 Gordon Research Conference on Radiation and Climate for helpful discussions.

References

Ackerman, A. S., O. B. Toon, D. E. Stevens, A. J. Heymsfield, V. Ramanathan, and E. J. Welton (2000), Reduction of tropical cloudiness by soot, *Science*, *288*(5468), 1042–1047.

Andreae, M. O., D. Rosenfeld, P. Artaxo, A. A. Costa, G. P. Frank, K. M. Longo, and M. A. F. Silva-Dias (2004), Smoking rain clouds over the Amazon, *Science*, *303*(5662), 1337–1342.

Cakmur, R. V., R. L. Miller, and I. Tegen (2001), A comparison of seasonal and interannual variability of soil dust aerosols over the Atlantic Ocean as inferred by the TOMS AI and AVHRR AOT retrievals, *J. Geophys. Res.*, *106*(D16), 18,287–18,303.

Chapman, E. G., W. J. Shaw, R. C. Easter, X. Bian, and S. J. Ghan (2002), Influence of wind speed averaging on estimates of dimethylsulfide emission fluxes, *J. Geophys. Res.*, *107*(D23), 4672, doi:10.1029/2001JD001564.

Charlson, R. J., J. E. Lovelock, M. O. Andreae, and S. G. Warren (1987), Oceanic phytoplankton, atmospheric sulfur, cloud albedo and climate, *Nature*, *326*(6114), 655–661.

Charlson, R. J., S. E. Schwartz, J. M. Hales, R. D. Cess, J. A. Coakley, J. E. Hansen, and D. J. Hofmann (1992), Climate forcing by anthropogenic aerosols, *Science*, *255*(5043), 423–430.

Chen, S. S., R. A. Houze, and B. E. Mapes (1996), Multiscale variability of deep convection in relation to large-scale circulation in TOGA COARE, *J. Atmos. Sci.*, *53*(10), 1380–1409.

Chu, D. A., Y. J. Kaufman, C. Ichoku, L. A. Remer, D. Tanre, and B. N. Holben (2002), Validation of MODIS aerosol optical depth retrieval over land, *Geophys. Res. Lett.*, *29*(12), 1617, doi:10.1029/2001GL013205.

de Graaf, M., P. Stammes, O. Torres, and R. B. A. Koelemeijer (2005), Absorbing aerosol index: Sensitivity analysis, application to GOME and comparison with TOMS, *J. Geophys. Res.*, *110*(D1), D01201, doi:10.1029/2004JD005178.

Eck, T. F., B. N. Holben, I. Slutsker, and A. Setzer (1998), Measurements of irradiance attenuation and estimation of aerosol single scattering albedo for biomass burning aerosols in Amazonia, *J. Geophys. Res.*, *103*(D24), 31,865–31,878.

Geogdzhayev, I. V., M. I. Mishchenko, W. B. Rossow, B. Cairns, and A. A. Lacis (2002), Global two-channel AVHRR retrievals of aerosol properties over the ocean for the period of NOAA-9 observations and preliminary retrievals using NOAA-7 and NOAA-11 data, *J. Atmos. Sci.*, *59*(3), 262–278.

Hansen, J., M. Sato, and R. Ruedy (1997), Radiative forcing and climate response, *J. Geophys. Res.*, *102*(D6), 6831–6864.

Haywood, J. M., P. N. Francis, I. Geogdzhayev, M. Mishchenko, and R. Frey (2001), Comparison of Saharan dust aerosol optical depths retrieved using aircraft mounted pyranometers and 2-channel AVHRR algorithms, *Geophys. Res. Lett.*, *28*(12), 2393–2396.

Hendon, H. H., and M. L. Salby (1994), The life-cycle of the Madden-Julian Oscillation, *J. Atmos. Sci.*, *51*(15), 2225–2237.

Herman, J. R., P. K. Bhartia, O. Torres, C. Hsu, C. Seftor, and E. Celarier (1997), Global distribution of UV-absorbing aerosols from Nimbus-7/TOMS data, *J. Geophys. Res.*, *102*(D14), 16,911–16,922.

Hobbs, P. V., J. S. Reid, R. A. Kotchenruther, R. J. Ferek, and R. Weiss (1997), Direct radiative forcing by smoke from biomass burning, *Science*, *275*(5307), 1777–1778.

Holben, B. N., et al. (1998), AERONET: A federated instrument network and data archive for aerosol characterization, *Remote Sens. Environ.*, *66*(1), 1–16.

Holben, B. N., et al. (2001), An emerging ground-based aerosol climatology: Aerosol optical depth from AERONET, *J. Geophys. Res.*, *106*(D11), 12,067–12,097.

Holben, B. N., T. F. Eck, I. Slutsker, A. Smirnov, A. Sinyuk, J. Schafer, D. Giles, and O. Dubovik (2006), AERONET's Version 2.0 quality assurance criteria, *Proc. SPIE Int. Soc. Opt. Eng.*, *6408*(64080Q), doi:10.1117/12.706524.

Hsu, N. C., J. R. Herman, P. K. Bhartia, C. J. Seftor, O. Torres, A. M. Thompson, J. F. Gleason, T. F. Eck, and B. N. Holben (1996), Detection of biomass burning smoke from TOMS measurements, *Geophys. Res. Lett.*, *23*(7), 745–748.

Hsu, N. C., J. R. Herman, J. F. Gleason, O. Torres, and C. J. Seftor (1999a), Satellite detection of smoke aerosols over a snow/ice surface by TOMS, *Geophys. Res. Lett.*, *26*(8), 1165–1168.

Hsu, N. C., J. R. Herman, O. Torres, B. N. Holben, D. Tanre, T. F. Eck, A. Smirnov, B. Chatenet, and F. Lavenu (1999b), Comparisons of the TOMS aerosol index with sun-photometer aerosol optical thickness: Results and applications, *J. Geophys. Res.*, *104*(D6), 6269–6279.

Husar, R. B., J. M. Prospero, and L. L. Stowe (1997), Characterization of tropospheric aerosols over the oceans with the NOAA advanced very high resolution radiometer optical thickness operational product, *J. Geophys. Res.*, *102*(D14), 16,889–16,909.

Ignatov, A., and N. R. Nalli (2002), Aerosol retrievals from the multiyear multisatellite AVHRR pathfinder atmosphere (PATMOS) dataset for correcting remotely sensed sea surface temperatures, *J. Atmos. Oceanic. Technol.*, *19*(12), 1986–2008.

Ignatov, A., J. Sapper, S. Cox, I. Laszlo, N. R. Nalli, and K. B. Kidwell (2004), Operational aerosol observations (AEROBS) from AVHRR/3 on board NOAA-KLM satellites, *J. Atmos. Oceanic. Technol.*, *21*(1), 3–26.

IPCC (2007), Climate change 2007: The physical science basis, in *Contribution of Working Group I to the Fourth Assessment Report of the Intergovernmental Panel on Climate Change*, 996 pp., Cambridge Univ. Press, New York.

Jeong, M.-J., and Z. Q. Li (2005a), Real effect or artifact of cloud cover on aerosol optical thickness?, paper presented at Fifteenth ARM Science Team Meeting, Daytona Beach, Fl., 14–18 Mar.

Jeong, M. J., and Z. Q. Li (2005b), Quality, compatibility, and synergy analyses of global aerosol products derived from the Advanced Very High Resolution Radiometer and Total Ozone Mapping Spectrometer, *J. Geophys. Res.*, *110*(D10), D10S08, doi:10.1029/2004JD004647.

Jeong, M. J., Z. Q. Li, D. A. Chu, and S. C. Tsay (2005), Quality and compatibility analyses of global aerosol products derived from the Advanced Very High Resolution Radiometer and Moderate Resolution Imaging Spectroradiometer, *J. Geophys. Res.*, *110*(D10), D10S09, doi:10.1029/2004JD004648.

Jeong, M.-J., Z. Q. Li, E. Andrews, and S.-C. Tsay (2007), Effect of aerosol humidification on the column aerosol optical thickness over the Atmospheric Radiation Measurement Southern Great Plains site, *J. Geophys. Res.*, *112*(D10), D10202, doi:10.1029/2006JD007176.

Jones, C., D. E. Waliser, K. M. Lau, and W. Stern (2004), Global occurrences of extreme precipitation and the Madden-Julian Oscillation: Observations and predictability, *J. Clim.*, *17*(23), 4575–4589.

Kahn, R. A., M. J. Garay, D. L. Nelson, K. K. Yau, M. A. Bull, B. J. Gaitley, J. V. Martonchik, and R. C. Levy (2007), Satellite-derived aerosol optical depth over dark water from MISR and MODIS: Comparisons with AERONET and implications for climatological studies, *J. Geophys. Res.*, *112*, D18205, doi:10.1029/2006JD008175.

Kaufman, Y. J., and I. Koren (2006), Smoke and pollution aerosol effect on cloud cover, *Science*, *313*(5787), 655–658.

Kaufman, Y. J., D. Tanre, L. A. Remer, E. F. Vermote, A. Chu, and B. N. Holben (1997), Operational remote sensing of tropospheric aerosol over land from EOS Moderate Resolution Imaging Spectroradiometer, *J. Geophys. Res.*, *102*(D14), 17,051–17,067.

Kaufman, Y. J., et al. (1998), Smoke, clouds, and radiation - Brazil (SCAR-B) experiment, *J. Geophys. Res.*, *103*(D24), 31,783–31,808.

Kaufman, Y. J., D. Tanre, and O. Boucher (2002a), A satellite view of aerosols in the climate system, *Nature*, *419*(6903), 215–223.

Kaufman, Y. J., D. Tanre, B. N. Holben, S. Mattoo, L. A. Remer, T. F. Eck, J. Vaughan, and B. Chatenet (2002b), Aerosol radiative impact on spectral solar flux at the surface, derived from principal-plane sky measurements, *J. Atmos. Sci.*, *59*(3), 635–646.

Kaufman, Y. J., et al. (2005), A critical examination of the residual cloud contamination and diurnal sampling effects on MODIS estimates of aerosol over ocean, *IEEE Trans. Geosci. Remote Sens.*, *43*(12), 2886–2897.

Kiehl, J. T., and B. P. Briegleb (1993), The relative roles of sulfate aerosols and greenhouse gases in climate forcing, *Science*, *260*(5106), 311–314.

Kiladis, G. N., G. A. Meehl, and K. M. Weickmann (1994), Large-scale circulation associated with westerly wind bursts and deep convection over the western equatorial Pacific, *J. Geophys. Res.*, *99*(D9), 18,527–18,544.

Kiladis, G. N., K. H. Straub, G. C. Reid, and K. S. Gage (2001), Aspects of interannual and intraseasonal variability of the tropopause and lower stratosphere, *Q. J. R. Meteorol. Soc.*, *127*(576), 1961–1983.

Kiladis, G. N., K. H. Straub, and P. T. Haertel (2005), Zonal and vertical structure of the Madden-Julian Oscillation, *J. Atmos. Sci.*, *62*(8), 2790–2809.

King, M. D., Y. J. Kaufman, D. Tanre, and T. Nakajima (1999), Remote sensing of tropospheric aerosols from space: Past, present, and future, *Bull. Am. Meteorol. Soc.*, *80*(11), 2229–2259.

Koch, D., J. Park, and A. Del Genio (2003), Clouds and sulfate are anticorrelated: A new diagnostic for global sulfur models, *J. Geophys. Res.*, *108*(D24), 4781, doi:10.1029/2003JD003621.

Koren, I., Y. J. Kaufman, L. A. Remer, and J. V. Martins (2004), Measurement of the effect of Amazon smoke on inhibition of cloud formation, *Science*, *303*(5662), 1342–1345.

Lau, W. K. M. (2005), ENSO connections, in *Intraseasonal Variability of the Atmosphere-Ocean Climate System*, edited by W. K. M. Lau and D. E. Waliser, pp. 271–306, Springer, New York.

Lau, K. M., and K. M. Kim (2006), Observational relationships between aerosol and Asian monsoon rainfall, and circulation, *Geophys. Res. Lett.*, *33*(21), L21810, doi:10.1029/2006GL027546.

Lau, W. K. M., and D. E. Waliser (Eds.) (2005), *Intraseasonal Variability of the Atmosphere-Ocean Climate System*, 474 pp., Springer, New York.

Levy, R. C., L. A. Remer, D. Tanre, Y. J. Kaufman, C. Ichoku, B. N. Holben, J. M. Livingston, P. B. Russell, and H. Maring (2003), Evaluation of the Moderate Resolution Imaging Spectroradiometer (MODIS) retrievals of dust aerosol over the ocean during PRIDE, *J. Geophys. Res.*, *108*(D19), 8594, doi:10.1029/2002JD002460.

Levy, R. C., L. A. Remer, J. V. Martins, Y. J. Kaufman, A. Plana-Fattori, J. Redemann, and B. Wenny (2005), Evaluation of the MODIS aerosol retrievals over ocean and land during CLAMS, *J. Atmos. Sci.*, *62*(4), 974–992.

Li, R. R., Y. J. Kaufman, W. M. Hao, J. M. Salmon, and B. C. Gao (2004), A technique for detecting burn scars using MODIS data, *IEEE Trans. Geosci. Remote Sens.*, *42*(6), 1300–1308.

Lin, X., and R. H. Johnson (1996), Kinematic and thermodynamic characteristics of the flow over the western Pacific warm pool during TOGA COARE, *J. Atmos. Sci.*, *53*(5), 695–715.

Lin, J.-L., M. H. Zhang, and B. Mapes (2005), Zonal momentum budget of the Madden-Julian Oscillation: The source and strength of equivalent linear damping, *J. Atmos. Sci.*, *62*(7), 2172–2188.

Lin, J. C., T. Matsui, R. A. Pielke, and C. Kummerow (2006), Effects of biomass-burning-derived aerosols on precipitation and clouds in the Amazon basin: A satellite-based empirical study, *J. Geophys. Res.*, *111*(D19), D19204, doi:10.1029/2005JD006884.

Loeb, N. G., and N. Manalo-Smith (2005), Top-of-atmosphere direct radiative effect of aerosols over global oceans from merged CERES and MODIS observations, *J. Clim.*, *18*(17), 3506–3526.

Madden, R. A., and P. R. Julian (1971), Detection of a 40–50 day oscillation in the zonal wind in the tropical Pacific, *J. Atmos. Sci.*, *28*(7), 702–708.

Madden, R. A., and P. R. Julian (1994), Observations of the 40–50-day tropical oscillation: A review, *Mon. Weather. Rev.*, *122*(5), 814–837.

Madden, R. A., and P. R. Julian (2005), Historical perspective, in *Intraseasonal Variability of the Atmosphere-Ocean Climate System*, edited by W. K. M. Lau and D. E. Waliser, pp. 1–18, Springer, New York.

Mahowald, N., C. Luo, J. del Corral, and C. S. Zender (2003), Interannual variability in atmospheric mineral aerosols from a 22-year model simulation and observational data, *J. Geophys. Res.*, *108*(D12), 4352, doi:10.1029/2002JD002821.

Maloney, E. D., and D. L. Hartmann (2000), Modulation of hurricane activity in the Gulf of Mexico by the Madden-Julian oscillation, *Science*, *287*(5460), 2002–2004, doi:10.1126/science.287.5460.2002.

Martins, J. V., D. Tanre, L. Remer, Y. Kaufman, S. Mattoo, and R. Levy (2002), MODIS cloud screening for remote sensing of aerosols over oceans using spatial variability, *Geophys. Res. Lett.*, *29*(12), 1619, doi:10.1029/2001GL013252.

Matheson, M. A., J. A. Coakley, and W. R. Tahnk (2005), Aerosol and cloud property relationships for summertime stratiform clouds in the northeastern Atlantic from Advanced Very High Resolution Radiometer observations, *J. Geophys. Res.*, *110*(D24), D24204, doi:10.1029/2005JD006165.

Mishchenko, M. I., and I. V. Geogdzhayev (2007), Satellite remote sensing reveals regional tropospheric aerosol trends, *Opt. Express*, *15*(12), 7423–7438.

Mishchenko, M. I., I. V. Geogdzhayev, B. Cairns, W. B. Rossow, and A. A. Lacis (1999), Aerosol retrievals over the ocean by use of channels 1 and 2 AVHRR data: Sensitivity analysis and preliminary results, *Appl. Opt.*, *38*(36), 7325–7341.

Myhre, G., et al. (2004), Intercomparison of satellite retrieved aerosol optical depth over the ocean, *J. Atmos. Sci.*, *61*(5), 499–513.

Myhre, G., et al. (2005), Intercomparison of satellite retrieved aerosol optical depth over ocean during the period September 1997 to December 2000, *Atmos. Chem. Phys.*, *5*, 1697–1719.

Ramanathan, V., P. J. Crutzen, J. T. Kiehl, and D. Rosenfeld (2001), Atmosphere-aerosols, climate, and the hydrological cycle, *Science*, *294*(5549), 2119–2124.

Redemann, J., P. B. Russell, and P. Hamill (2001), Dependence of aerosol light absorption and single-scattering albedo on ambient relative humidity for sulfate aerosols with black carbon cores, *J. Geophys. Res.*, *106*(D21), 27,485–27,495.

Remer, L. A., et al. (2002), Validation of MODIS aerosol retrieval over ocean, *Geophys. Res. Lett.*, *29*(12), 1618, doi:10.1029/2001GL013204.
Remer, L. A., et al. (2005), The MODIS aerosol algorithm, products, and validation, *J. Atmos. Sci.*, *62*(4), 947–973.
Rosenfeld, D. (1999), TRMM observed first direct evidence of smoke from forest fires inhibiting rainfall, *Geophys. Res. Lett.*, *26*(20), 3105–3108.
Rosenfeld, D. (2000), Suppression of rain and snow by urban and industrial air pollution, *Science*, *287*(5459), 1793–1796.
Rossow, W. B., and L. C. Garder (1993), Cloud detection using satellite measurements of infrared and visible radiances for ISCCP, *J. Clim.*, *6*(12), 2341–2369.
Rossow, W. B., and R. A. Schiffer (1999), Advances in understanding clouds from ISCCP, *Bull. Am. Meteorol. Soc.*, *80*(11), 2261–2287.
Rui, H., and B. Wang (1990), Development characteristics and dynamic structure of tropical intraseasonal convection anomalies, *J. Atmos. Sci.*, *47*(3), 357–379.
Satheesh, S. K., and V. Ramanathan (2000), Large differences in tropical aerosol forcing at the top of the atmosphere and Earth's surface, *Nature*, *405*(6782), 60–63.
Smirnov, A., B. N. Holben, T. F. Eck, O. Dubovik, and I. Slutsker (2000), Cloud-screening and quality control algorithms for the AERONET database, *Remote Sens. Environ.*, *73*(3), 337–349.
Smirnov, A., B. N. Holben, T. F. Eck, O. Dubovik, and I. Slutsker (2003), Effect of wind speed on columnar aerosol optical properties at Midway Island, *J. Geophys. Res.*, *108*(D24), 4802, doi:10.1029/2003JD003879.
Tanre, D., Y. J. Kaufman, M. Herman, and S. Mattoo (1997), Remote sensing of aerosol properties over oceans using the MODIS/EOS spectral radiances, *J. Geophys. Res.*, *102*(D14), 16,971–16,988.
Tian, B. J., D. E. Waliser, and E. J. Fetzer (2006a), Modulation of the diurnal cycle of tropical deep convective clouds by the MJO, *Geophys. Res. Lett.*, *33*(20), L20704, doi:10.1029/2006GL027752.
Tian, B. J., D. E. Waliser, E. J. Fetzer, B. H. Lambrigtsen, Y. L. Yung, and B. Wang (2006b), Vertical moist thermodynamic structure and spatial-temporal evolution of the MJO in AIRS observations, *J. Atmos. Sci.*, *63*(10), 2462–2485.
Tian, B. J., Y. L. Yung, D. E. Waliser, T. Tyranowski, L. Kuai, E. J. Fetzer, and F. W. Irion (2007), Intraseasonal variations of the tropical total ozone and their connection to the Madden-Julian Oscillation, *Geophys. Res. Lett.*, *34*, L08704, doi:10.1029/2007GL029451.
Torres, O., P. K. Bhartia, J. R. Herman, Z. Ahmad, and J. Gleason (1998), Derivation of aerosol properties from satellite measurements of backscattered ultraviolet radiation: Theoretical basis, *J. Geophys. Res.*, *103*(D14), 17,099–17,110.
Torres, O., A. Tanskanen, B. Veihelman, C. Ahn, R. Braak, P. K. Bhartia, P. Veefkind, and P. Levelt (2007), Aerosols and surface UV products from ozone monitoring instrument observations: An overview, *J. Geophys. Res.*, *112*, D24S47, doi:10.1029/2007JD008809.
Twomey, S. A., M. Piepgrass, and T. L. Wolfe (1984), An assessment of the impact of pollution on global cloud albedo, *Tellus, Ser. B*, *36*(5), 356–366.
Vecchi, G. A., and N. A. Bond (2004), The Madden-Julian Oscillation (MJO) and northern high latitude wintertime surface air temperatures, *Geophys. Res. Lett.*, *31*(4), L04104, doi:10.1029/2003GL018645.
Waliser, D. E. (2006a), Intraseasonal variability, in *The Asian Monsoon*, edited by B. Wang, pp. 203–257, Springer, New York.
Waliser, D. E. (2006b), Predictability of tropical intraseasonal variability, in *Predictability of Weather and Climate*, edited by T. N. Palmer and R. Hagedorn, p. 718, Cambridge Univ. Press, New York.
Waliser, D. E., R. Murtugudde, and L. Lucas (2003), Indo-Pacific ocean response to atmospheric intraseasonal variability: 1. Austral summer and the Madden-Julian Oscillation, *J. Geophys. Res.*, *108*(C5), 3160, doi:10.1029/2002JC001620.
Waliser, D. E., R. Murtugudde, P. Strutton, and J.-L. Li (2005), Subseasonal organization of ocean chlorophyll: Prospects for prediction based on the Madden-Julian Oscillation, *Geophys. Res. Lett.*, *32*, L23602, doi:10.1029/2005GL024300.
Wang, B., and H. Rui (1990), Synoptic climatology of transient tropical intraseasonal convection anomalies-1975–1985, *Meteorol. Atmos. Phys.*, *44*(1–4), 43–61.
Weare, B. C., and J. S. Nasstrom (1982), Examples of extended empirical orthogonal function analyses, *Mon. Weather Rev.*, *110*, 481–485.
Wen, G. Y., R. F. Cahalan, S. C. Tsay, and L. Oreopoulos (2001), Impact of cumulus cloud spacing on Landsat atmospheric correction and aerosol retrieval, *J. Geophys. Res.*, *106*(D11), 12,129–12,138.
Wen, G. Y., A. Marshak, and R. F. Cahalan (2006), Impact of 3-D clouds on clear-sky reflectance and aerosol retrieval in a biomass burning region of Brazil, *IEEE Geosci. Remote Sens.*, *3*(1), 169–172.
Wen, G. Y., A. Marshak, R. F. Cahalan, L. A. Remer, and R. G. Kleidman (2007), 3-D aerosol-cloud radiative interaction observed in collocated MODIS and ASTER images of cumulus cloud fields, *J. Geophys. Res.*, *112*, D13204, doi:10.1029/2006JD008267.
Wheeler, M. C., and J. L. McBride (2005), Australian-Indonesian monsoon, in *Intraseasonal Variability of the Atmosphere-Ocean Climate System*, edited by W. K. M. Lau and D. E. Waliser, pp. 125–174, Springer, New York.
Wilcox, E. M., and V. Ramanathan (2004), The impact of observed precipitation upon the transport of aerosols from South Asia, *Tellus, Ser. B*, *56*(5), 435–450.
Wong, S., and A. E. Dessler (2007), Regulation of H2O and CO in tropical tropopause layer by the Madden-Julian Oscillation, *J. Geophys. Res.*, *112*(D14), D14305, doi:10.1029/2006JD007940.
Xie, P. P., and P. A. Arkin (1997), Global precipitation: A 17-year monthly analysis based on gauge observations, satellite estimates, and numerical model outputs, *Bull. Am. Meteorol. Soc.*, *78*(11), 2539–2558.
Yu, H., et al. (2006), A review of measurement-based assessments of the aerosol direct radiative effect and forcing, *Atmos. Chem. Phys.*, *6*, 613–666.
Zhang, C. (2005), The Madden-Julian Oscillation, *Rev. Geophys.*, *43*, RG2003, doi:10.1029/2004RG000158.
Zhang, J. L., J. S. Reid, and B. N. Holben (2005), An analysis of potential cloud artifacts in MODIS over ocean aerosol optical thickness products, *Geophys. Res. Lett.*, *32*(15), L15803, doi:10.1029/2005GL023254.

I. V. Geogdzhayev and M. I. Mishchenko, NASA Goddard Institute for Space Studies, 2880 Broadway, New York, NY 10025, USA.
R. A. Kahn, NASA Goddard Space Flight Center, Code 613.2, Greenbelt, MD 20771, USA.
Q. Li and D. E. Waliser, Jet Propulsion Laboratory, California Institute of Technology, M/S 183-501, 4800 Oak Grove Drive, Pasadena, CA 91109, USA.
A. Smirnov, Sciences Systems and Applications, Inc., 10210 Greenbelt Rd., Ste. 600, Lanham, MD 20706, USA.
B. Tian, Joint Institute for Regional Earth System Science and Engineering, University of California, 9258 Boelter Hall, Box 957228, Los Angeles, CA 90095-7228, USA. (baijun.tian@jpl.nasa.gov)
O. Torres, Joint Center for Earth Systems Technology, University of Maryland Baltimore County, Suite 320, 5523 Research Park Drive, Baltimore, MD 21228, USA.
T. Tyranowski and Y. L. Yung, Division of Geological and Planetary Sciences, California Institute of Technology, MC 170-25, 1200 E. California Blvd., Pasadena, CA 91125, USA.